Available online at www.sciencedirect.com
SCIENCE DIRECT
International Journal of Heat and Mass Transfer 49 (2006) 1137–1147
International Journal of HEAT and MASS TRANSFER
www.elsevier.com/locate/ijhmt

Inverse analysis for estimating the unsteady inlet temperature distribution for two-phase laminar flow in a channel

Yun Ky Hong, Seung Wook Baek *

Division of Aerospace Engineering, Department of Mechanical Engineering, Korea Advanced Institute of Science and Technology, 373-1 Guseong-dong, Yuseong-gu, Daejeon 305-701, Republic of Korea

Received 10 November 2004
Available online 24 October 2005

Abstract

An inverse thermal problem was considered for two-phase laminar flow in a parallel plate duct. The inlet temperature, which varies temporally as well as spatially, was estimated when measured temperatures were available at downstream of the duct. In the present study, the problem is solved through a minimization of an objective function by using two regularization methods, i.e., the iterative conjugate gradient method (CGM) and the Tikhonov regularization method (TRM). The effects of the functional form of inlet temperature profile, the number of the measurement points and the measurement errors are investigated and discussed. The computational accuracy and efficiency of these two regularization method are compared and discussed.

Keywords: Inverse convection problem; Two-phase; Conjugate gradient method; Tikhonov regularization method

1. Introduction

The inverse heat transfer problems have numerous applications in various branches of science and engineering, but the inverse problem cannot be directly solved due to their ill-posed nature. The ill-posed nature renders many algorithms used for direct problems inapplicable to inverse problems, so that special numerical techniques must be employed to stabilize the results. Among others, commonly used technique is the regularization method. There are two kinds of regularization method, the conjugate gradient method (CGM) and the Tikhonov regularization method (TRM). The CGM solves the inverse problem in iterative manner. It requires a solution of the direct problem, the sensitivity problem and the adjoint problem [1]. On the other hand, the TRM is a procedure which modifies the objective function by adding smoothing factors that reduce the influence of measurement errors [2].

Whereas the inverse conduction problem can be found quite often in the literatures or books, but the inverse convection problem is relatively less. Huang and Özisik [3] solved the inverse convection problem to estimate the wall heat flux in laminar and forced convection flow from the temperature measurement in the domain. They solved it using CGM with adjoint problem and sensitivity problem while neglecting the axial conduction. For the same condition, Liu and Özisik [4] considered the inverse convection problem to estimate the spatially varying inlet temperature profile in the laminar duct flow. The temporally varying inlet temperature profile was predicted from the temperature measurement by Bokar and Özisik [5]. In 1996, Liu and Özisik [6] extended the inverse convection problem to the turbulent forced convection problem. The problem of a timewise and spacewise variation of the wall heat flux was unraveled by Machado and Orlande [7] in a parallel plate channel.

Until now, many inverse heat convection problems including the above mentioned literatures have been related to the one-phase flow. In this study, however, two-phase laminar flow is considered so that the gas temperature is

* Corresponding author. Tel.: +82 42 869 3714; fax: +82 42 869 3710.
E-mail addresses: shineyk@kaist.ac.kr (Y.K. Hong), swbaek@kaist.ac.kr (S.W. Baek).

0017-9310/$ - see front matter © 2005 Elsevier Ltd. All rights reserved.
doi:10.1016/j.ijheatmasstransfer.2005.07.051

Nomenclature

A_p	particle's surface area, m^2
c	specific heat, J/(kg K)
d_p	particle's diameter, m
$\mathbf{d}^k$	direction of descent at kth iteration, Eq. (13)
f_p	particle's volume fraction
F	inlet temperature distribution
h	convective heat transfer coefficient
H	height of duct
H_0	regularization matrix, Eq. (23)
J	the number of points which are to be determined
k_g	conductivity, W/(m K)
L	duct length
M	the number of sensors
N_p	number density of particle, m^{-3}
Nu	non-dimensional variable, Eq. (3j)
Nu_H	non-dimensional variable, Eq. (3k)
Pe	non-dimensional variable, Eqs. (3h) and (3i)
Re	non-dimensional variable, Eq. (3g)
S	objective function, Eq. (5)
T	temperature, K
ΔT	sensitivity function satisfying problem (6)
u	velocity, m/s
Y	measured temperature, K
Z	sensitivity coefficient, Eq. (26)
$\mathbf{Z}$	sensitivity matrix, Eq. (25)

Greek symbols

β^k	search step size at kth iteration, Eq. (15)
$\delta()$	Dirac delta function
ε	convergence criterion
γ	regularization parameter
γ^k	conjugation coefficient at kth iteration, Eq. (14)
λ, ξ	Langrange multiplier satisfying problem (8)
Θ	non-dimensional temperature
ρ	density, kg/m^3
σ	standard deviation
ω	random number

Superscripts

k	number of iteration
*	non-dimensional variable
0	guessed value

Subscripts

g	gas
in	inlet
j	jth boundary point
m	mth measurement point
out	outlet
p	particle
w	wall

in thermal non-equilibrium with the particle temperature. Inlet temperature, which varies temporally as well as spatially, is determined by using two regularization methods mentioned above, given temperature measurements at downstream in the domain.

2. Formulation

2.1. Conjugate gradient method

2.1.1. Direct problem

In this study two-phase laminar flow, which is composed of air and stainless steel in a parallel plate duct, is considered as schematized in Fig. 1. Stainless steel particles are assumed uniformly distributed with spherical shape. Thermo-fluid dynamic properties of gas and particles are assumed to be temperature-independent. No energy dissipation due to viscosity is taken into account due to low velocity. Initial gas and particle temperatures are T_0 at $t = 0$, while a temporal temperature variation of $F(t,y)$ is applied at inlet, $x = 0$ for $t > 0$. These two-phase temperature are then cooled by wall temperature T_w to reach the equilibrium temperature T_w at far downstream.

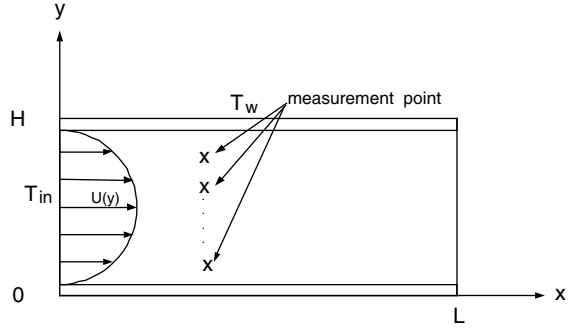

Fig. 1. Schematic of the problem.

A set of governing equations for gas and particle phases are given by [8]

$$\rho_g(1-f_p)c_g\left(\frac{\partial T_g}{\partial t}+u\frac{\partial T_g}{\partial x}\right) = k_g\left(\frac{\partial^2 T_g}{\partial x^2}+\frac{\partial^2 T_g}{\partial y^2}\right)-hA_pN_p(T_g-T_p) \tag{1a}$$

$$T_g(t,0,y)=T_{in}=F(t,y) \tag{1b}$$

$$T_g(t,x,0)=T_w \tag{1c}$$

$$T_g(t,x,H)=T_w \tag{1d}$$

$$T_g(t,L,y)=T_w \tag{1e}$$

$$T_g(t=0,x,y)=T_0 \tag{1f}$$

$$\rho_p f_p c_p\left(\frac{\partial T_p}{\partial t}+u\frac{\partial T_p}{\partial x}\right)=-hA_pN_p(T_p-T_g) \tag{1g}$$

$$T_p(t,0,y)=T_{in}=F(t,y) \tag{1h}$$

$$T_p(t=0,x,y)=T_0 \tag{1i}$$

where the fully developed velocity [9] is represented by

$$\frac{u}{u_{\text{mean}}} = 6\left(\frac{y}{H} - \left(\frac{y}{H}\right)^2\right) \tag{2}$$

By introducing the following non-dimensional variables:

$$t^* = \frac{t}{H/u_{\text{mean}}}, \quad x^* = \frac{x}{H}, \quad y^* = \frac{y}{H},$$
$$\Theta_{\text{g}} = \frac{T_{\text{g}} - T_{\text{w}}}{T_{\max} - T_{\text{w}}}, \quad \Theta_{\text{p}} = \frac{T_{\text{p}} - T_{\text{w}}}{T_{\max} - T_{\text{w}}}, \tag{3a–e}$$
$$u^* = \frac{u}{u_{\text{mean}}} = 6y^*(1-y^*), \quad Re = \frac{u_{\text{mean}} H}{\upsilon},$$
$$Pe_{\text{g}} = RePr = \frac{u_{\text{mean}} H \rho_{\text{g}} c_{\text{g}}}{k_{\text{g}}}, \tag{3f–h}$$
$$Pe_{\text{p}} = \frac{u_{\text{mean}} H \rho_{\text{p}} c_{\text{p}}}{k_{\text{g}}}, \quad Nu = \frac{h d_{\text{p}}}{k_{\text{g}}}, \quad Nu_H = \frac{h d_{\text{p}}}{k_{\text{g}}} \times \frac{H}{d_{\text{p}}} = \frac{hH}{k_{\text{g}}},$$
$$A_{\text{p}}^* = \frac{A_{\text{p}}}{H^2}, \quad N_{\text{p}}^* = N_{\text{p}} H^3 \tag{3i–m}$$

The set of governing equations in non-dimensional variables are obtained as

$$Pe_{\text{g}}(1-f_{\text{p}})\left(\frac{\partial \Theta_{\text{g}}}{\partial t^*} + u^* \frac{\partial \Theta_{\text{g}}}{\partial x^*}\right) = \left(\frac{\partial^2 \Theta_{\text{g}}}{\partial x^{*2}} + \frac{\partial^2 \Theta_{\text{g}}}{\partial y^{*2}}\right) - Nu_H A_{\text{p}}^* N_{\text{p}}^* (\Theta_{\text{g}} - \Theta_{\text{p}}) \tag{4a}$$
$$\Theta_{\text{g}}(t^*, 0, y^*) = \Theta_{\text{in}} \tag{4b}$$
$$\Theta_{\text{g}}(t^*, x^*, 0) = \Theta_{\text{w}} \tag{4c}$$
$$\Theta_{\text{g}}(t^*, x^*, 1) = \Theta_{\text{w}} \tag{4d}$$
$$\Theta_{\text{g}}\left(t^*, \frac{L}{H}, y^*\right) = \Theta_{\text{w}} \tag{4e}$$
$$\Theta_{\text{g}}(t^* = 0, x^*, y^*) = \Theta_0 \tag{4f}$$
$$Pe_{\text{p}} f_{\text{p}}\left(\frac{\partial \Theta_{\text{p}}}{\partial t^*} + u^* \frac{\partial \Theta_{\text{p}}}{\partial x^*}\right) = -Nu_H A_{\text{p}}^* N_{\text{p}}^* (\Theta_{\text{p}} - \Theta_{\text{g}}) \tag{4g}$$
$$\Theta_{\text{p}}(t^*, 0, y^*) = \Theta_{\text{in}} \tag{4h}$$
$$\Theta_{\text{p}}(t^* = 0, x^*, y^*) = \Theta_0 \tag{4i}$$

From now on, non-dimensional variables are expressed without an asterisk and non-dimensional temperature Θ_{g} and Θ_{p} will be expressed as T_{g} and T_{p} for convenience.

2.1.2. Inverse problem

For the inverse problem the inlet temperature profile $F(t,y)$ is regarded as unknown and is to be estimated by using the temperature measurements of M sensors located at appropriate locations (x_m, y_m), $m = 1, \ldots, M$ inside the duct. The CGM is applied to minimize the following functional:

$$S(F(t,y)) = \int_{t=0}^{t=t_f} \sum_{m=1}^{M} [Y_{\text{m}}(t,x,y) - T_{\text{g}}(t, x_m, y_m; F(t,y))]^2 \, \text{d}t \tag{5}$$

where, Y_{m} and T_{g} are measured and estimated gas temperature at the measurement locations. The estimated temperature T_{g} is the solution of the direct problem by assuming the inlet temperature profile $F(t,y)$. Two auxiliary problems are also required for the successful implementation of the CGM: the Sensitivity Problem and the Adjoint Problem.

2.1.3. Sensitivity problem

To obtain the sensitivity problem, it is assumed in the direct problem that when $F(t,y)$ undergoes a small increment $\Delta F(t,y)$, the temperature T_{g} and T_{p} change by ΔT_{g} and ΔT_{p}. Therefore, by replacing $F(t,y)$ by $F(t,y) + \Delta F(t,y)$, T_{g} by $T_{\text{g}} + \Delta T_{\text{g}}$ and T_{p} by $T_{\text{p}} + \Delta T_{\text{p}}$ in the direct problem (4) and then subtracting Eqs. (4) from it, the following sensitivity problem is obtained:

$$Pe_{\text{g}}(1-f_{\text{p}})\left(\frac{\partial \Delta T_{\text{g}}}{\partial t} + u \frac{\partial \Delta T_{\text{g}}}{\partial x}\right) = \left(\frac{\partial^2 \Delta T_{\text{g}}}{\partial x^2} + \frac{\partial^2 \Delta T_{\text{g}}}{\partial y^2}\right) - Nu_H A_{\text{p}} n_{\text{p}} (\Delta T_{\text{g}} - \Delta T_{\text{p}}) \tag{6a}$$
$$\Delta T_{\text{g}}(t, 0, y) = \Delta F(t,y) \tag{6b}$$
$$\Delta T_{\text{g}}(t, x, 0) = 0 \tag{6c}$$
$$\Delta T_{\text{g}}(t, x, 1) = 0 \tag{6d}$$
$$\Delta T_{\text{g}}\left(t, \frac{L}{H}, y\right) = 0 \tag{6e}$$
$$\Delta T_{\text{g}}(t = 0, x, y) = 0 \tag{6f}$$
$$Pe_{\text{p}} f_{\text{p}}\left(\frac{\partial \Delta T_{\text{p}}}{\partial t} + u \frac{\partial \Delta T_{\text{p}}}{\partial x}\right) = -Nu_H A_{\text{p}} n_{\text{p}} (\Delta T_{\text{p}} - \Delta T_{\text{g}}) \tag{6g}$$
$$\Delta T_{\text{p}}(t, 0, y) = \Delta F(y) \tag{6h}$$
$$\Delta T_{\text{p}}(t = 0, x, y) = 0 \tag{6i}$$

2.1.4. Adjoint problem and gradient equation

To derive the adjoint problem, Eqs. (4a) and (4g) are multiplied by the Lagrange multipliers $\lambda(t,x,y)$ and $\xi(t,x,y)$. The resulting expression is integrated over the time and space domain, and then added to the right-hand side of Eq. (5) to yield

$$\begin{aligned} S(F(t,y)) = {} & \int_{t=0}^{t=t_f} \sum_{m=1}^{M} [Y_{\text{m}}(t,x,y) - T_{\text{g}}(t, x_m, y_m; F(t,y))]^2 \, \text{d}t \\ & + \int_{t=0}^{t=t_f} \int_{x=0}^{L} \int_{y=0}^{H} \lambda(x,y) \left[-Pe_{\text{g}}(1-f_{\text{p}}) \left(\frac{\partial T_{\text{g}}}{\partial t} + u \frac{\partial T_{\text{g}}}{\partial x}\right) \right. \\ & \left. + \left(\frac{\partial^2 T_{\text{g}}}{\partial x^2} + \frac{\partial^2 T_{\text{g}}}{\partial y^2}\right) - Nu_H A_{\text{p}} N_{\text{p}} (T_{\text{g}} - T_{\text{p}}) \right] \text{d}x \, \text{d}y \, \text{d}t \\ & + \int_{t=0}^{t=t_f} \int_{x=0}^{L} \int_{y=0}^{H} \xi(x,y) \left[-Pe_{\text{p}} f_{\text{p}} \left(\frac{\partial T_{\text{p}}}{\partial t} + u \frac{\partial T_{\text{p}}}{\partial x}\right) \right. \\ & \left. - Nu_H A_{\text{p}} N_{\text{p}} (T_{\text{p}} - T_{\text{g}}) \right] \text{d}x \, \text{d}y \, \text{d}t \end{aligned} \tag{7}$$

Next, the variation $\Delta S[F(t,y))$ of Eq. (7) is obtained. After some algebraic manipulations, the resulting expressions are allowed to go to zero. From them, the following adjoint problem is obtained for the determination of the Lagrange multiplier $\lambda(t,x,y)$ and $\xi(t,x,y)$

$$Pe_g(1-f_p)\left(\frac{\partial\lambda}{\partial t}+u\frac{\partial\lambda}{\partial x}\right)+\left(\frac{\partial^2\lambda}{\partial x^2}+\frac{\partial^2\lambda}{\partial y^2}\right)-Nu_H A_p N_p(\lambda-\xi)+\sum_{m=1}^{M}2[T_g-Y]\delta(x-x_m)\delta(y-y_m)=0 \tag{8a}$$

$$\lambda(t,0,y)=0 \tag{8b}$$

$$\lambda(t,x,0)=0 \tag{8c}$$

$$\lambda(t,x,1)=0 \tag{8d}$$

$$\lambda\left(t,\frac{L}{H},y\right)=0 \tag{8e}$$

$$\lambda(t=t_f,x,y)=0 \tag{8f}$$

$$Pe_p f_p\left(\frac{\partial\xi}{\partial t}+u\frac{\partial\xi}{\partial x}\right)-Nu_H A_p N_p(\xi-\lambda)=0 \tag{8g}$$

$$\xi\left(t,\frac{L}{H},y\right)=0 \tag{8h}$$

$$\xi(t=t_f,x,y)=0 \tag{8i}$$

where $\delta()$ is the Dirac delta function and the variation $\Delta S[F(t,y)]$ is determined as

$$\Delta S[F(t,y)]=\int_{t=0}^{t=t_f}\int_{y=0}^{1}\left\{Pe_p f_p u\xi(t,0,y)+\frac{\partial\lambda(t,0,y)}{\partial x}\right\}\Delta F(t,y)\,dy\,dt \tag{9}$$

We note that $\Delta S[F(t,y)]$, by definition, is given by

$$\Delta S[F(t,y)]=\int_{t=0}^{t=t_f}\int_{y=0}^{1}\nabla S[F(t,y)]\Delta F(t,y)\,dy\,dt \tag{10}$$

From comparison of Eq. (2.9) with (2.10), we conclude that

$$\nabla S[F(t,y)]=Pe_p f_p u\xi(t,0,y)+\left.\frac{\partial\lambda}{\partial x}\right|_{t,0,y} \tag{11}$$

This is the gradient equation that relates the gradient of the functional $S(F(t,y))$ to the Lagrange multiplier $\lambda(t,x,y)$ and $\xi(t,x,y)$.

2.1.5. Iterative procedure

Assuming that the functions T_g, T_p, ΔT_g, ΔT_p, $\lambda(t,x,y)$, $\xi(t,x,y)$ and $\nabla S[F(t,y)]$ are available at the kth iteration, the iterative procedure is performed as follows. The boundary temperature at step $k+1$ is computed from

$$F^{k+1}(t,y)=F^k(t,y)-\beta^k\mathbf{d}^k(t,y) \tag{12}$$

where $\mathbf{d}^k$ is the direction of descent, determined from

$$\mathbf{d}^k=\nabla S[F^k(t,y)]+\gamma^k\mathbf{d}^{k-1} \tag{13}$$

and the conjugation coefficient γ^k is obtained from the Fletcher–Reeves expression [1] as

$$\gamma^k=\frac{\int_{t=0}^{t=t_f}\int_{y=0}^{y=1}\left\{\nabla S[F^k(t,y)]\right\}^2 dy\,dt}{\int_{t=0}^{t=t_f}\int_{y=0}^{y=1}\left\{\nabla S[F^{k-1}(t,y)]\right\}^2 dy\,dt}\quad\text{with }\gamma^0=0 \tag{14}$$

The search step size β^k is obtained by minimizing the functional given by Eq. (5) with respect to β^k such that

$$\beta^k=\frac{\int_{t=0}^{t=t_f}\sum_{m=1}^{M}[T_g(t,x_m,y_m;F^k(t,y))-Y_m]\Delta T_g(t,x_m,y_m;\mathbf{d}^k)\,dt}{\int_{t=0}^{t=t_f}\sum_{m=1}^{M}[\Delta T_g(x_m,y_m;\mathbf{d}^k)]^2\,dt} \tag{15}$$

where $\Delta T_g(t,x_m,y_m;\mathbf{d}^k)$ is the solution of the sensitivity problem (6) which is obtained by setting $\Delta F(t,y)=\mathbf{d}^k$.

2.1.6. Discrepancy principle for stopping criterion

If the problem contains no measurement error, the traditional check condition is specified as

$$S(F^{k+1}(t,y))<\varepsilon \tag{16}$$

where the value of the tolerance ε is chosen so that sufficiently stable solutions are obtained. However the observed temperature data contains measurement errors. As the estimated temperatures approach the measured temperatures containing errors, a large oscillation may appear during the minimization of the function (5) in the inverse solution, resulting in an ill-posed nature character for the inverse problem. However, the CGM may become well-posed if the discrepancy principle is used to stop the iterative procedure. When the residuals between measured and estimated temperatures are of the same order of magnitude of σ such that

$$|Y(t_{measured},x_{measured},y_{measured})-T(t_{measured},x_{measured},y_{measured})|\approx\sigma \tag{17}$$

where σ is the standard deviation of the measurements which is assumed to be a constant, the following expression is obtained for stopping criteria ε by substituting Eq. (17) into Eq. (5)

$$\varepsilon=\sum_{m=1}^{M}\int_{t=0}^{t=t_f}\sigma^2\,dt=Mt_f\sigma^2 \tag{18}$$

Then the stopping criterion is given by Eq. (16) with ε determined from Eq. (18).

2.1.7. Computational procedure

Suppose an initial guess $F^0(t,y)$ is available for the function $F(t,y)$. Set $k=0$ and then

Step 1. Solve the direct problem in order to compute T_g and T_p.

Step 2. Check the stopping criterion. Continue if not satisfied.

Step 3. With T_g and measured temperature Y_m, solve the adjoint problem (8) and obtain variable $\lambda(t,x,y)$ and $\xi(t,x,y)$.

Step 4. With $\lambda(t,x,y)$ and $\xi(t,x,y)$, compute the gradient vector $\nabla S[F^k(t,y)]$ from Eq. (11).

Step 5. With the gradient $\nabla S[F^k(t,y)]$, compute γ^k from Eq. (14). Then compute the direction of descent $\mathbf{d}^k$ from Eq. (13).

Step 6. Set $\Delta F^k = \mathbf{d}^k$ and solve the sensitivity problem (6) to obtain $\Delta T_g(t,x,y;\mathbf{d}^k)$.

Step 7. With $\Delta T_g(t,x,y;\mathbf{d}^k)$, compute the search step size β^k from Eq. (15).

Step 8. With the search step size β^k and the direction of the descent $\mathbf{d}^k$, compute the new estimate $F^{k+1}(t,y)$ from Eq. (12). And return to Step 1.

2.2. Tikhonov regularization method

2.2.1. Direct problem

The direct problem would be the same as that for conjugate gradient method.

2.2.2. Inverse problem

The objective of this method is to minimize the following functional

$$S(F(t,y)) = \int_{t=0}^{t=t_f} \sum_{m=1}^{M} [Y_m(t,x,y) - T_g(t,x_m,y_m;F(t,y))]^2 \,\mathrm{d}t \tag{19}$$

Here, the objective function can be modified by adding the following regularization term

$$\gamma \|\mathbf{F}\|^2 \tag{20}$$

where γ is called the regularization parameter. It is determined by using L-curve method [10,11]. The L-curve method is sketched in the following:

Define the following curve

$$L = \{(\phi\|\mathbf{F}\|^2), \phi(S(F(t,y))) : \gamma > 0\} \tag{21}$$

The curve is known as L-curve and a suitable regularization parameter γ corresponds to a regularized solution near the 'corner' of the L-curve.

Regularization term must be discretized and added to the objective function, yielding

$$S(F(t,y)) = (\mathbf{Y} - \mathbf{T}_g)^{\mathrm{T}}(\mathbf{Y} - \mathbf{T}_g) + \gamma(\mathbf{H}_0\mathbf{F})^{\mathrm{T}}(\mathbf{H}_0\mathbf{F}) \tag{22}$$

The square matrix $\mathbf{H}_0$ is referred to as a regularization matrix.

$$\mathbf{H}_0 = \mathbf{I} \quad (\mathbf{I} : J \times J \text{ indentity matrix}) \tag{23}$$

The boundary temperature can be found by minimizing $S(F(t,y))$ which can be accomplished by matrix differentiation with respect to the unknowns, yielding

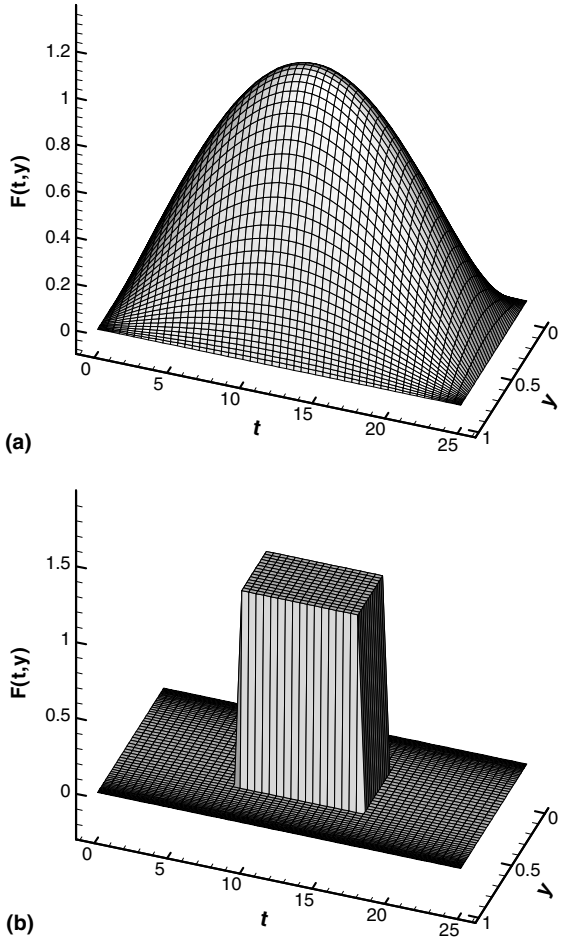

Fig. 2. Two test cases. (a) Sinusoidal variation. (b) Stepwise variation.

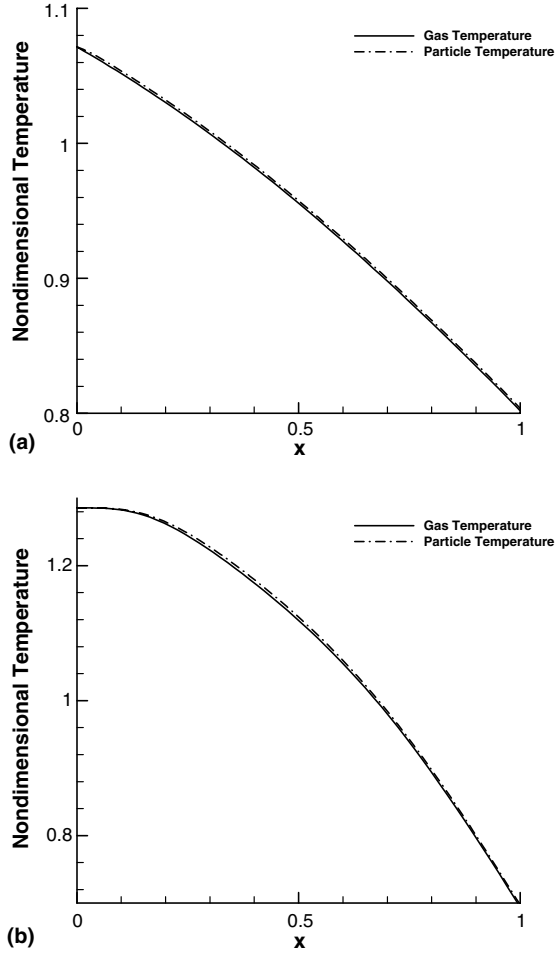

Fig. 3. Temperature difference between gas and particle. (a) Test (1). (b) Test (2).

$$\{\mathbf{Z}^{\mathrm{T}}\mathbf{Z}+\gamma\mathbf{H}_0^{\mathrm{T}}\mathbf{H}_0\}\mathbf{F}=\mathbf{Z}^{\mathrm{T}}(\mathbf{Y}-\mathbf{T}_{\mathrm{g}}^0)+\mathbf{Z}^{\mathrm{T}}\mathbf{Z}\mathbf{F}^0 \tag{24}$$

where $\mathbf{Z}$ is the sensitivity matrix which is expressed by following expression.

$$\mathbf{Z}=\begin{bmatrix} (\mathbf{Z}_{\mathrm{g}})_1^1 & \cdots & (\mathbf{Z}_{\mathrm{g}})_1^j & \cdots & (\mathbf{Z}_{\mathrm{g}})_1^J \\ \cdots & \cdots & \cdots & \cdots & \cdots \\ (\mathbf{Z}_{\mathrm{g}})_m^1 & \cdots & (\mathbf{Z}_{\mathrm{g}})_m^j & \cdots & (\mathbf{Z}_{\mathrm{g}})_m^J \\ \cdots & \cdots & \cdots & \cdots & \cdots \\ (\mathbf{Z}_{\mathrm{g}})_M^1 & \cdots & (\mathbf{Z}_{\mathrm{g}})_M^j & \cdots & (\mathbf{Z}_{\mathrm{g}})_M^J \end{bmatrix} \tag{25}$$

2.2.3. Sensitivity coefficient

Sensitivity matrix is composed of sensitivity coefficients. Each sensitivity coefficient is defined by

$$(Z_{\mathrm{g}})_m^j=\frac{\partial(T_{\mathrm{g}})_m}{\partial F_j},\quad (Z_{\mathrm{p}})_m^j=\frac{\partial(T_{\mathrm{p}})_m}{\partial F_j}\quad j=1\text{–}J,\ m=1\text{–}M \tag{26}$$

where j refers to the boundary point associated with the unknown inlet temperature, whereas m refers to interior location of measurement point.

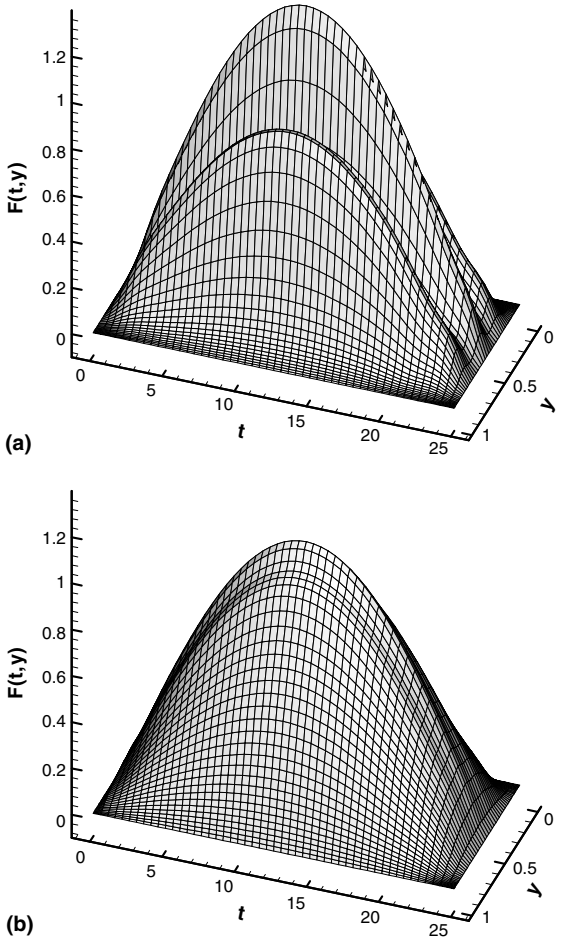

Fig. 4. Results obtained by conjugate gradient method for $\sigma=0.0$ K. Number of measurement points = 5 (a) and 11 (b).

The equation set of them can be obtained by differentiation of the direct problem (4) with respect to the unknown boundary temperature $F(t,y)$, which gives

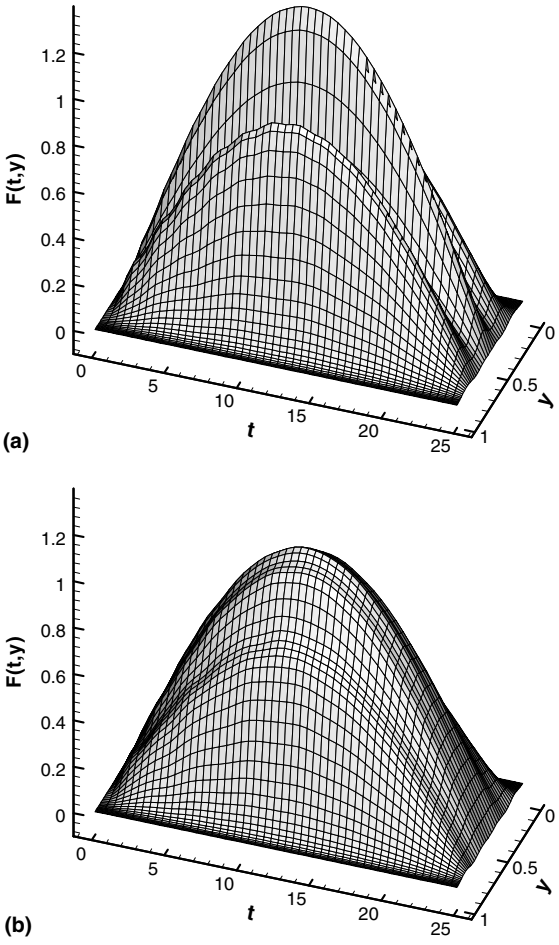

Fig. 5. Results obtained by Tikhonov regularization method for $\sigma=0.0$ K. Number of measurement points = 5 ($\gamma=1.68\times10^{-3}$) (a) and 11 ($\gamma=1.008\times10^{-3}$) (b).

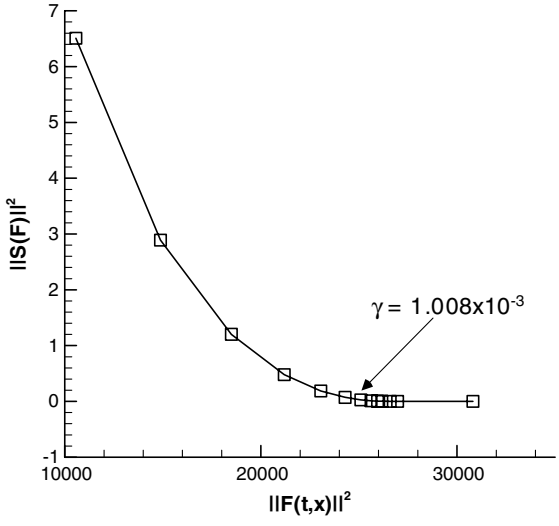

Fig. 6. The L-curve for the test case (1) for 11 measurement points and $\sigma=0.0$ K.

$$Pe_g(1-f_p)\left(\frac{\partial(Z_g)^j}{\partial t}+u\frac{\partial(Z_g)^j}{\partial x}\right)=\left(\frac{\partial^2(Z_g)^j}{\partial x^2}+\frac{\partial^2(Z_g)^j}{\partial y^2}\right) - Nu_H A_p n_p((Z_g)^j-(Z_p)^j) \quad (27a)$$

$$(Z_g)^j(t,0,y)=\begin{cases}1, & \text{if } y \text{ belongs to position of } j\\ 0, & \text{otherwise}\end{cases} \quad (27b)$$

$$(Z_g)^j(t,x,0)=0 \quad (27c)$$

$$(Z_g)^j(t,x,1)=0 \quad (27d)$$

$$(Z_g)^j\left(t,\frac{L}{H},y\right)=0 \quad (27e)$$

$$(Z_g)^j(t=0,x,y)=0 \quad (27f)$$

$$Pe_p f_p\left(\frac{\partial(Z_p)^j}{\partial t}+u\frac{\partial(Z_p)^j}{\partial x}\right)=-Nu_H A_p n_p((Z_p)^j-(Z_g)^j) \quad (27g)$$

$$(Z_p)^j(t,0,y)=\begin{cases}1, & \text{if } y \text{ belongs to position of } j\\ 0, & \text{otherwise}\end{cases} \quad (27h)$$

$$(Z_p)^j(t=0,x,y)=0 \quad (27i)$$

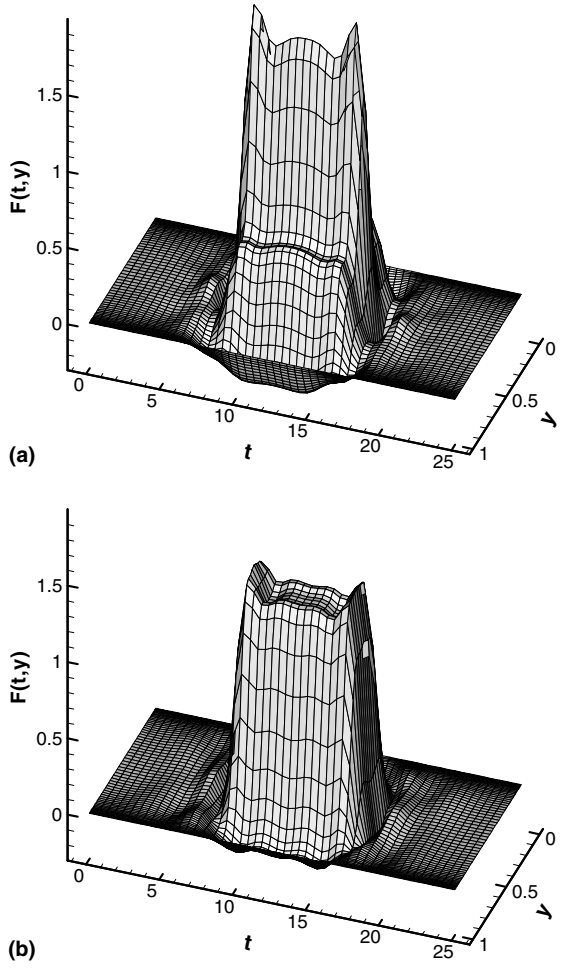

Fig. 7. Results obtained by conjugate gradient method for $\sigma = 0.0$ K. Number of measurement points = 5 (a) and 11 (b).

2.2.4. Computational procedure

Step 1. Calculate sensitivity coefficient from Eqs. (27) and construct sensitivity matrix **Z**.
Step 2. Assume the initial value for the regularization parameter γ.
Step 3. Set $F^0(t,y)=0$ as an initial value.
Step 4. Calculate T_g from Eqs. (4).
Step 5. With sensitivity matrix **Z** and estimated temperature T_g at measuring points, calculate $F(t,y)$ from Eq. (24) for various values of regularization parameter γ.
Step 6. Determine the complete temperature distribution from Eqs. (4).

3. Results and discussion

The computational accuracy and efficiency of the present inverse analysis is examined in estimating the unknown inlet temperature profile. Two test cases have been considered with simulated measurements $Y_{measured}$ which includes some artificial measurement errors. The estimated inlet temperature is then compared with the exact one without any measurement error. The channel length is taken long

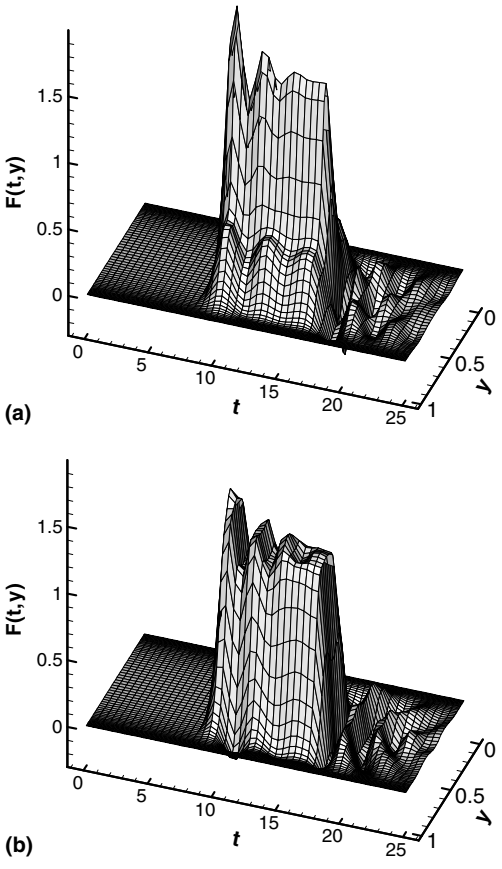

Fig. 8. Results obtained by Tikhonov regularization method for $\sigma = 0.0$ K. Number of measurement points = 5 ($\gamma = 2.16\times10^{-2}$) (a) and 11 ($\gamma = 1.296\times10^{-2}$) (b).

enough to cover the thermally developing region such that L is 50 m and H is 0.2 m. And the sensors are placed at the downstream location, $x = 0.2$ m from the inlet. The air properties are $\rho_g = 0.4975$ kg/m^3, $c_g = 1075$ J/kg K and $\kappa_g = 0.0524$ W/m K. The properties of stainless steel particle used here are $\rho_p = 8238$ kg/m^3, $c_p = 563$ J/kg K and $\kappa_p = 19.8$ W/m K. And the diameter of particle is $d_p = 100$ μm with volume fraction, $f_p = 5.23 \times 10^{-7}$. The mean flow velocity, u_{mean}, is 0.1 m/s [8]. The heat transfer coefficient h is assumed to be 2.0 W/m^2 K.

The simulated measured temperature data, $Y_{measured}$, are generated by adding some random errors to the computed exact temperatures as follows:

$$Y_{measured} = T_{exact} + \omega\sigma \tag{28}$$

where σ is the selected standard deviation which takes values of 4.0 K and 8.0 K, and ω is a random number between $-2.576 \leqslant \omega \leqslant 2.576$ which represents 99% confidence bound for the measured temperature.

Two types of equations for $F(t,y)$ are selected for the test cases as shown in Fig. 2:

$$(1)\ F(t,y) = 1.071\sin(\pi y) \times \sin\left(\pi\frac{t}{t_f}\right) \tag{29a}$$

$$(2)\ \begin{matrix} F(t,y) = 9/7 & (0.3 < y < 0.7, 8 < t < 17) \\ F(t,y) = 0 & (\text{elsewhere}) \end{matrix} \tag{29b}$$

Here, y and t is non-dimensional variables. The test case (1) has sinusoidal variation, while the test case (2) has stepwise variation of the inlet temperature profile.

Fig. 3 shows the two-phase temperature variation along the centerline of the channel up to 1 m from the inlet when the time is equal to 12.5. Since the gas is cooled by the wall first and then the particle is cooled by the gas, the particle temperature is observed to be higher than that of gas. If the particle's volume fraction decreases, the temperature difference would further increase.

In order to estimate the effect of number of measurement points on the accuracy, an idealized situation, in which there is no measurement error, i.e., $\sigma = 0.0$ K, is considered. Figs. 4 and 5 show the estimated inlet temperature $F(t,y)$ for the test case (1) when CGM and TRM are, respectively, employed. The numbers of measurement points used are 5 and 11. When TRM is applied to the inverse problem, the regularization parameter has to be determined. Fig. 6 shows the L-curve and regularization

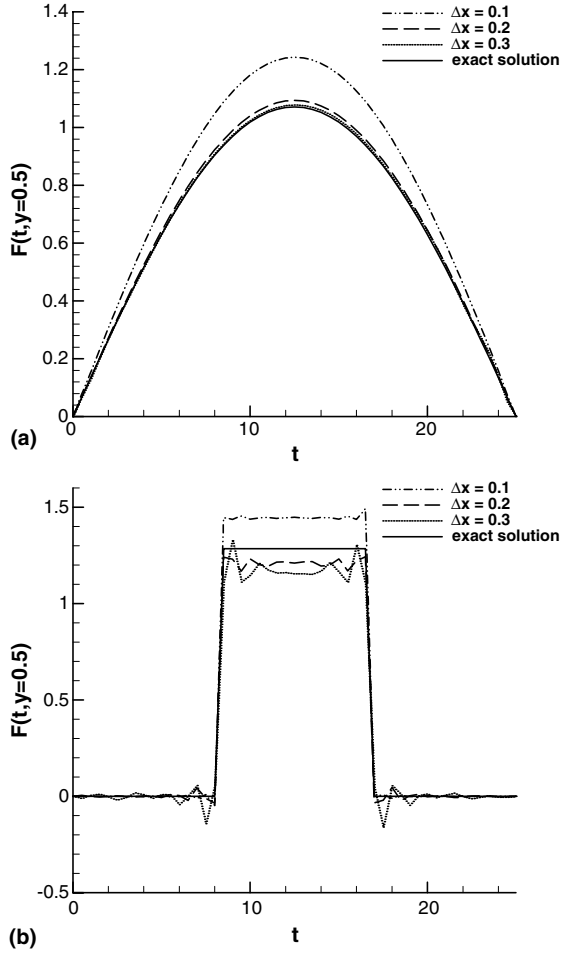

Fig. 9. Effect of measurement position using conjugate gradient method with $M = 11$. (a) Test case (1). (b) Test case (2).

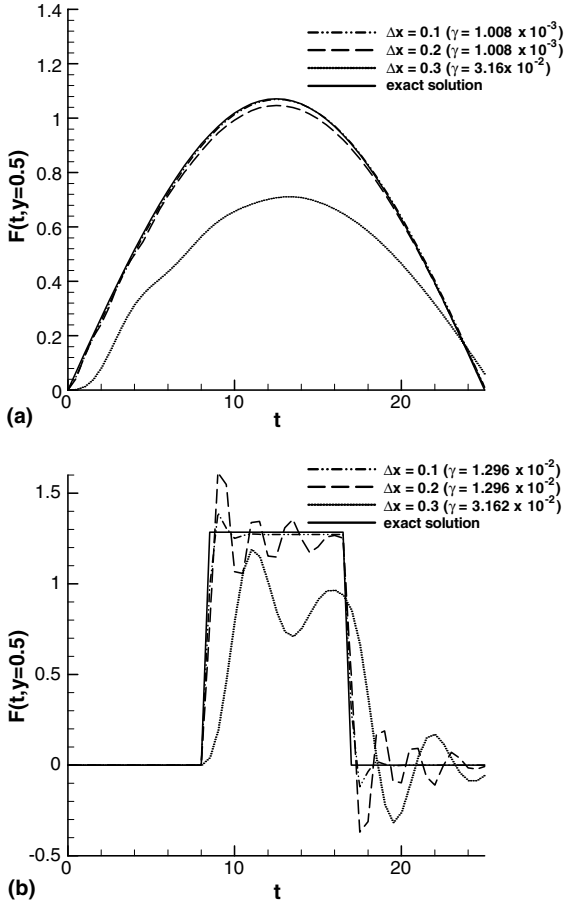

Fig. 10. Effect of measurement position using Tikhonov regularization method with $M = 11$. (a) Test case (1). (b) Test case (2).

parameter, $\gamma = 1.008 \times 10^{-3}$, for the test case (1) when the number of measurement points is 11. In this figure, the regularization parameter corresponds to the corner of the L-curve. When the number of measurement points is 5, the regularization parameter becomes 1.68×10^{-3} which is higher than previous one. This higher regularization value represents that more regularization is required to control the ill-posed characteristics. It is taken for granted that the estimated inlet temperature is more accurate when the number of measurement points is 11. Temporal as well as spatial variation of temperature is shown to be well predicted by both CGM and TRM, since no measurement error is involved.

Figs. 7 and 8 illustrate the estimated inlet temperature for the test case (2). These figures also show that both CGM and TRM yield better results when the number of measurement point is 11. But some wiggling behavior is observed in the results due to its inherent discontinuity in the step function. Based on this fact, discontinuous function estimation is considered more difficult to inversely analyze.

In order to find the effect of measurement position, more results obtained by CGM and TRM are plotted in Figs. 9 and 10 for various measurement positions. These results are obtained for the case which has 11 measurement points and no measurement error. Figs. 9 and 10 show the estimated inlet temperature distribution along the height of the duct. Here, Δx denotes the downstream measurement position from the duct inlet. According to Fig. 9, it can be found that the CGM's results are less accurate when the measurement position is shifted toward the inlet. CGM uses the gradient information to find the inlet temperature. Since the hot flow starts to cool fast from the inlet, its gradient is large therein, it becomes harder to accurately estimate inlet temperature. However, for the test case (2) with step variation in temperature, it can be found that when the measurement position is located far from the inlet, there is more oscillation in solution near the discontinuity. The results for TRM show that the estimated inlet temperature becomes more accurate when the measurement position is near the inlet. This is because TRM uses the sensitivity coefficients which are larger near the inlet.

Now, the case with measurement error is to be considered. The results with measurement error $\sigma = 4.0$ and 8.0 K are plotted in Figs. 11–14 for the number of measurement points of 11. Fig. 11(a) and (b) show the results obtained by using the CGM for the test case (1) with the measurement error $\sigma = 4.0$ K and $\sigma = 8.0$ K, while Fig. 12(a) and (b) represent the results by TRM for the same test case with measurement error $\sigma = 4.0$ K and $\sigma = 8.0$ K. Figs. 13 and 14 are the results for the test case (2) when CGM and TRM is employed. According to the figures, it can be found that the results for two test cases

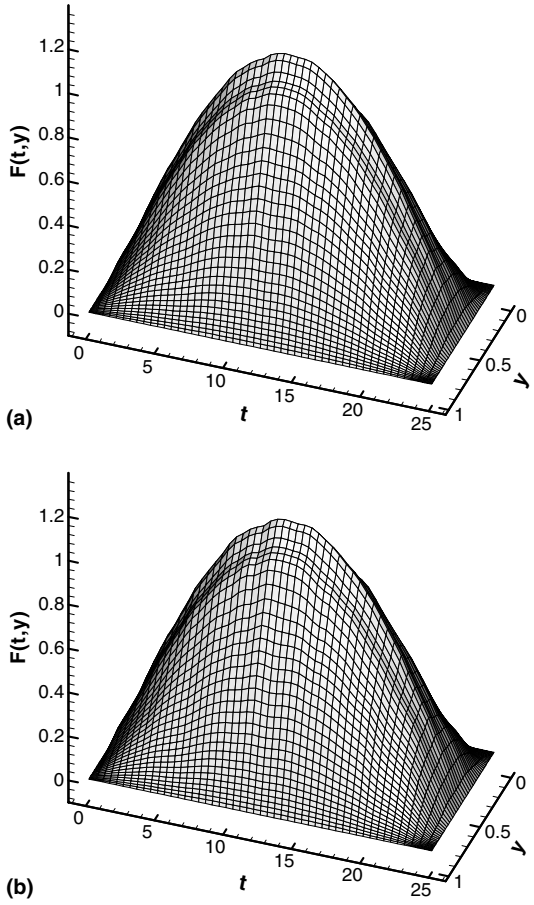

Fig. 11. Effect of measurement error using conjugate gradient method with $M = 11$. Standard deviation of measurement error = 4.0 K (a) and 8.0 K (b).

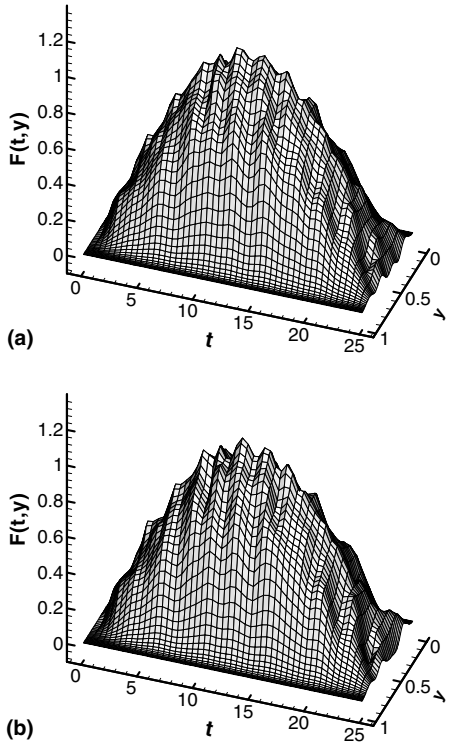

Fig. 12. Effect of measurement error using Tikhonov regularization method with $M = 11$. Standard deviation of measurement error = 4.0 K ($\gamma = 7.776 \times 10^{-3}$) (a) and 8.0 K ($\gamma = 1.296 \times 10^{-2}$) (b).

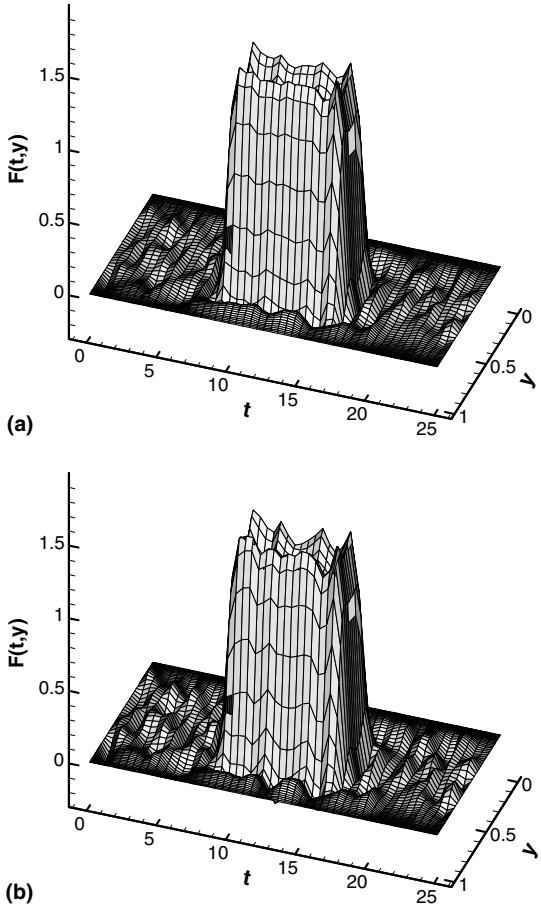

Fig. 13. Effect of measurement error using conjugate gradient method with $M = 11$. Standard deviation of measurement error = 4.0 K (a) and 8.0 K (b).

with the measurement error $\sigma = 4.0$ K are better than those for the cases with measurement error $\sigma = 8.0$ K. It is also noted that TRM produces poorer results than the iterative method, CGM as observed from the wiggling behavior in the figures. The results in temporal as well as spatial variation of temperature for the test case (2), which are attained by TRM for $\sigma = 8.0$ K, are the worst, but they still show stepwise variation.

To compare two regularization methods more precisely, the accuracy and computational time of CGM and TRM are listed in Tables 1 and 2 for two cases for which there are measurement errors involved.

The average error for the inlet temperature profile in Table 1 is defined as [12]

$$\text{Average error } (\%) = \left[\sum_{t=1}^{t=t_f}\sum_{j=1}^{J}\left|\frac{F(t,y)-\widehat{F}(t,y)}{F(t,y)}\right|\right] \Big/ (J \times t_f) \times 100\% \qquad (30)$$

where $F(t,y)$ and $\widehat{F}(t,y)$ denote the exact and estimated values of inlet temperature and J denotes the total number of boundary points which have to be determined.

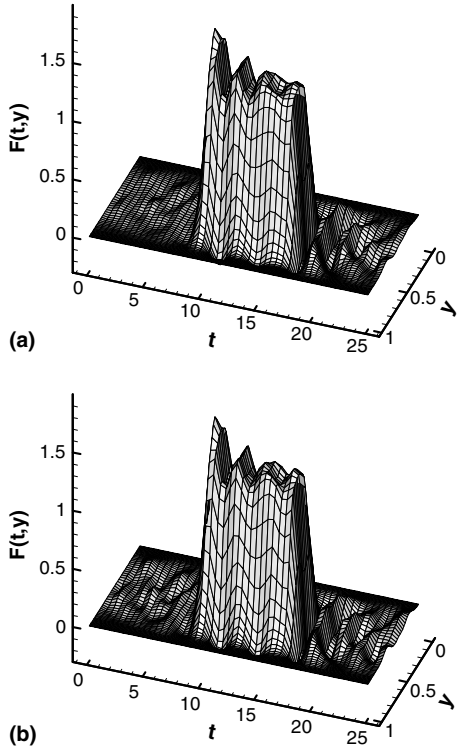

Fig. 14. Effect of measurement error using Tikhonov regularization method with $M = 11$. Standard deviation of measurement error = 4.0 K ($\gamma = 1.296 \times 10^{-2}$) (a) and 8.0 K ($\gamma = 1.296 \times 10^{-2}$) (b).

Table 1
Comparison of average error (%)

Method/σ	Case (1)	Case (2)
CGM/4.0 K	0.82	7.03
CGM/8.0 K	1.13	7.94
TRM/4.0 K	6.54	8.14
TRM/8.0 K	7.40	8.53

Table 2
Comparison of computing time (s)

Method/σ	Case (1)	Case (2)
CGM/4.0 K	3446	15,835
CGM/8.0 K	2172	13,384
TRM/4.0 K	12,787	12,770
TRM/8.0 K	12,790	12,785

When CGM is used, the average error for the test case (1) is 0.82% and 1.13%, respectively, for $\sigma = 4.0$ and $\sigma = 8.0$ K. But when TRM is employed, the average error is increased to 6.54% and 7.40% for the same test case. For the test case (2), the average error of CGM is 7.03% and 7.94%, while that of TRM is 8.14% and 8.53%. Based on these results, the accuracy of CGM is observed to be better than that of TRM.

The computational time is also calculated and compared for each case in Table 2. The computer used for calculation is equipped with a CPU of Pentium 4 1.5 GHz. For the

case of CGM, it takes longer time when the measurement error is small. For example, the computing time for test case (1) and case (2) is 3446 and 15,835 s for the measurement error $\sigma = 4.0$ K. However, for $\sigma = 8.0$ K, it becomes 2172 and 13,384 s for the same test cases. This is because the stopping criterion ε becomes smaller for smaller measurement error due to discrepancy principle. Also, the computing time for test case (2) is longer than that for test case (1). Actually, it takes three iterations for measurement error of 4.0 K and two iterations for measurement error of 8.0 K to get convergent solutions. But for the test case (2), it takes 12 iterations and 10 iterations, respectively, for $\sigma = 4.0$ and $\sigma = 8.0$ K. From these results, it can be found that CGM needs more iterations and computing time when the unknown distribution has discontinuity. For the case of TRM, it takes almost the same computing time, i.e., about 12,785 s, for all the cases. This is because TRM spends most of computing time to calculate the sensitivity coefficients which are common for all the cases. Based on these, if the unknown temperature distribution has no discontinuity, usually CGM takes a shorter computing time than TRM, since the conjugate gradient method with adjoint problem does not need to calculate the sensitivity coefficient. But, if there is a discontinuity in the unknown temperature distribution, the CGM takes much computing time than the TRM which does not need to iterate, because CGM needs more iterations for convergence.

4. Conclusions

In this study, two regularization methods, the conjugate gradient method and the Tikhonov regularization method are used to solve the inverse heat transfer problem for determining the unknown inlet temperature in two-phase laminar flow, when measured temperature is available at downstream of the channel.

The conjugate gradient method with the adjoint problem, which is one of iterative regularization methods, was found to provide a more accurate solution than the Tikhonov regularization method. But the computing time of CGM strongly depends on the functional form of unknowns, because this inverse method usually needs some iterations to solve the inverse problem. On the other hand, the Tikhonov regularization method requires almost the same computing time regardless of the functional form of unknowns because in this problem it does not need iterations to solve the inverse problem. Instead, this method necessitates a calculation of sensitivity coefficients which requires a long computational time.

It was also found that these regularization methods, both CGM and TRM, have more difficulties in calculation, when the unknown temperature profile has a discontinuity in distribution, thereby inevitably introducing more inaccuracy in the solution.

Acknowledgements

The present work was supported by the Combustion Engineering Research Center at the Department of Mechanical Engineering, Korea Advanced Institute of Science and Technology, which is funded by the Korea Science and Engineering Foundation.

References

[1] M.N. Özisik, Helcio R.B. Orlande, Inverse Heat Transfer, Taylor and Francis, New York, 2000 [Chapters 1–4].
[2] K. Kurpisz, A.J. Nowak, Inverse Thermal Problems, Computational Mechanics Publications, Southampton, UK and Boston, USA, 1995 [Chapters 1–5].
[3] C.H. Huang, M.N. Özisik, Inverse problem of determining unknown wall heat in laminar flow through a parallel plate, Numer. Heat Transfer, Part A 21 (1992) 55–70.
[4] F.B. Liu, M.N. Özisik, Estimation of inlet temperature profile in laminar duct flow, Inverse Prob. Eng. 3 (1996) 131–141.
[5] J.C. Bokar, M.N. Özisik, Inverse analysis for estimating the time varying inlet temperature in laminar flow inside a parallel plate duct, Int. J. Heat Mass Transfer 38 (1995) 39–45.
[6] F.B. Liu, M.N. Özisik, Inverse analysis of transient turbulent forced convection inside parallel plates, Int. J. Heat Mass Transfer 39 (1996) 2615–2618.
[7] H.A. Machado, Helcio R.B. Orlande, Inverse analysis of estimating the timewise and spacewise variation of the wall heat flux in a parallel plate channel, Int. J. Heat Mass Transfer 7 (1997) 696–710.
[8] H.J. Lee, Analysis of Combined Heat Transfer of Gas-Particle Two-Phase Media, MS thesis, Korea Advanced Institute of Science and Technology, Daejeon, Republic of Korea, 1998.
[9] I.G. Currie, Fundamental Mechanics of Fluids, second ed., McGraw-Hill, Inc., Singapore, 1993, pp. 220–222.
[10] Y.C. Hon, T. Wei, A fundamental solution method for inverse heat conduction problem, Eng. Anal. Bound. Elem. 28 (2004) 489–495.
[11] D. Dalvetti, S. Morigi, L. Reichel, F. Sgallari, Tikhonov regularization and the *L*-curve for large discrete ill-posed problems, J. Comput. Appl. Math. 123 (2000) 423–446.
[12] C.H. Huand, W.C. Chen, A three-dimensional inverse forced convection problem in estimation surface heat flux by conjugate gradient method, Int. J. Heat Mass Transfer 43 (2000) 3171–3181.